



Attique, S., Batool, M., Goerke, O., Abbas, G., Saeed, F. A., Din, M. I., Jalees, I., Ahmad, I., Gregory, D. H. and Shah, A. T. (2022) Fe-POM/ attapulgate composite materials: efficient catalysts for plastic pyrolysis. *Waste Management and Research*, (doi: 10.1177/0734242X221080084)

There may be differences between this version and the published version. You are advised to consult the publisher's version if you wish to cite from it.

<https://eprints.gla.ac.uk/264206/>

Deposited on: 28 January 2022

Enlighten – Research publications by members of the University of Glasgow
<https://eprints.gla.ac.uk>

Fe-POM/ Attapulgite Composite Materials: Efficient catalysts for plastic pyrolysis

Journal:	<i>Waste Management & Research: The Journal for a Sustainable Circular Economy</i>
Manuscript ID	WMR-21-0732.R1
Manuscript Type:	Original article: 35,000 characters
Date Submitted by the Author:	29-Nov-2021
Complete List of Authors:	Attique, Saira; University of the Punjab Quaid-i-Azam Campus, Institute of Chemistry Batool, Madeeha; University of the Punjab Quaid-i-Azam Campus, Institute of Chemistry Goerke, Oilver; Technical University of Berlin, Department of Ceramic Materials Abbas, Ghayur; The Islamia University of Bahawalpur Pakistan Saeed, Faraz; COMSATS Institute of Information Technology - Lahore Campus Din, Muhammad; University of the Punjab Quaid-i-Azam Campus, Institute of Chemistry Jalees, Irfan; University of Engineering and Technology Ahmad, Irfan; King Khalid University Gregory, Duncan; University of Glasgow, WestCHEM, School of Chemistry Tufail Shah, Asma; COMSATS Institute of Information Technology - Lahore Campus,
Keywords:	Waste recycling, Pyrolysis, Tungstophosphate, Liquid Hydrocarbon, Polyethylene, GC-MS, Clay
Abstract:	This manuscript describes the catalytic cracking of low-density polyethylene over attapulgite clay and iron substituted tungstophosphate/attapulgite clay (Fe-POM/attapulgite) composite materials to evaluate their suitability and performance for recycling of plastic waste into liquid fuel. These catalysts enhanced the yield of liquid fuel (hydrocarbons) produced in cracking process. A maximum yield of 82% liquid oil fraction with a negligible amount of coke was obtained for 50% Fe-POM/attapulgite composite.. Whereas, only 68% liquid oil fractions with a large amount of solid black residue was produced in case of non-catalytic pyrolysis. Moreover, Fe-POM/attapulgite clay composites showed higher selectivity towards lower hydrocarbons (C5–C12) with aliphatic hydrocarbons as major fractions. These synthesized composite catalysts significantly lowered the pyrolysis temperature The from 375 °C to 310 °C. Hence, recovery of valuable fuel oil from polyethylene using these synthesized catalysts suggested their applicability for energy production from plastic waste at industrial level as well as for effective environment pollution control.

1
2
3
4
5
6
7
8
9
10
11
12
13
14
15
16
17
18
19
20
21
22
23
24
25
26
27
28
29
30
31
32
33
34
35
36
37
38
39
40
41
42
43
44
45
46
47
48
49
50
51
52
53
54
55
56
57
58
59
60

Fe-POM/ Attapulgit Composite Materials: Efficient catalysts for plastic pyrolysis

Saira Attique¹, Madeeha Batool¹, Oliver Goerke², Ghayoor Abbas³, Faraz Ahmad Saeed⁴, Muhammad Imran Din¹, Irfan Jalees⁵, Irfan Ahmad⁶, Duncan H. Gregory⁷, Asma Tufail Shah^{2,8†}

¹Institute of Chemistry, University of the Punjab, New Campus, Lahore-54000, Pakistan

²Fachgebiet Keramische Werkstoffe/Chair of Advanced Ceramic Materials, Technische Universität Berlin, Hardenbergstr. 40, 10623 Berlin, Germany

³Faculty of Pharmacy and Alternative Medicine, Islamia University Bahawalpur, Bahawalpur, Pakistan

⁴Ahmad Saeed & Co Pvt. Ltd. 473 G3, Johar Town, Lahore, 54000, Pakistan

⁵Institute of Environmental Engineering And Research, University of Engineering and Technology, Lahore 54890, Pakistan

⁶Department of Chemistry, College of Science, King Khalid University, Abha, Saudi Arabia

⁷WestCHEM, School of Chemistry, Joseph Black Building, University of Glasgow, Glasgow, G12 8QQ, United Kingdom

⁸Interdisciplinary Research Centre in Biomedical Materials (IRCBM), COMSATS University Islamabad, Lahore Campus, Lahore-54600, Pakistan

Corresponding Author:

1. Dr. Asma Tufail Shah

Telephone # +92 (0) 42-111-001-007 Ext. 828

Fax: +92-42-35321090

Email: drasmashah@cuilahore.edu.pk

2. Dr. Madeeha Batool

Email: madeeha.chem@pu.edu.pk

Abstract

This manuscript describes the catalytic cracking of low-density polyethylene over attapulgite clay and iron substituted tungstophosphate/attapulgite clay (Fe-POM/attapulgite) composite materials to evaluate their suitability and performance for recycling of plastic waste into liquid fuel. These catalysts enhanced the yield of liquid fuel (hydrocarbons) produced in cracking process. A maximum yield of 82% liquid oil fraction with a negligible amount of coke was obtained for 50% Fe-POM/attapulgite composite. Whereas, only 68% liquid oil fractions with a large amount of solid black residue was produced in case of non-catalytic pyrolysis. Moreover, Fe-POM/attapulgite clay composites showed higher selectivity towards lower hydrocarbons (C_5 – C_{12}) with aliphatic hydrocarbons as major fractions. These synthesized composite catalysts significantly lowered the pyrolysis temperature from 375 °C to 310 °C. Hence, recovery of valuable fuel oil from polyethylene using these synthesized catalysts suggested their applicability for energy production from plastic waste at industrial level as well as for effective environment pollution control.

Keywords: Waste recycling; Pyrolysis; Tungstophosphate; Liquid Hydrocarbon; Polyethylene; GC-MS.

Introduction

Thermal and thermo-catalytic degradation of waste polymers into valuable hydrocarbons, like fuel oil, is an area of great interest due to depletion of natural resources (Gaca, Drzewiecka et al. 2008). Thermal degradation requires a very high temperature (500 °C – 900 °C). It produces

1
2
3 liquid products that mainly contain heavier hydrocarbons ($C_6 - C_{25}$) (Lin, Yang et al. 2004,
4 Akpanudoh, Gobin et al. 2005). The use of catalyst not only decreases the degradation temperature
5 but also maximizes the yield of lower hydrocarbons (Bobek-Nagy, Gao et al. 2020, Chai, Wang et
6 al. 2020, Shah, Attique et al. 2021). Various catalysts including, silica, alumina, zeolites,
7 mesoporous materials, and heteropolyacids have been tested for polymer degradation to get
8 valuable hydrocarbons (Serrano, Aguado et al. 2000, Mastral, Berrueco et al. 2006, Aguado,
9 Serrano et al. 2007, Shah, Attique et al. 2021, Wang, Jiang et al. 2021). Heteropolyacids, also
10 known as polyoxometalates (POMs), have been reported for catalytic cracking of plastic. POMs
11 are molecular metal oxide clusters that possess larger number of Brønsted acid sites that accelerate
12 the cracking process (Shah, Attique et al. 2021).
13
14
15
16
17
18
19
20
21
22
23
24
25

26 Natural clays have acidic sites which made them suitable for catalytic applications. Various
27 types of clays, such as bentonite, smectite, montmorillonite, and kaolin have been used as a
28 catalyst/support due to their porosity, active surface elements. They have good thermal stability
29 which ensures their use in applications at high temperature. Kaolin and Fire clay had been reported
30 for catalytic cracking of polyethylene with liquid yield 73 % and 43 %, respectively (Patil, Varma
31 et al. 2018, Saira Attique 2018). Wei Luo et al. reported kaolin clay for pyrolysis of PE at 600 °C
32 to get liquid and oil products (Luo, Fan et al. 2021). Clays impregnated with POMs had been
33 reported to enhance oil yield upto 81 % (Saira Attique 2018, Attique, Batool et al. 2020). Thus,
34 POM increase the polymer conversion that in turn enhances the liquid oil formation that is more
35 useful fuel.
36
37
38
39
40
41
42
43
44
45
46
47
48
49
50

51 In the present study, attapulgite clay has been impregnated with Cs salt of iron substituted
52 POM (tungstophosphate) to develop highly efficient acidic cracking catalyst. Attapulgite is a
53 hydrated magnesium-aluminum silicate material that consists of tetrahedrally arranged double
54
55
56
57

1
2
3 chains of silica interconnected by octahedral oxygen and hydroxyl groups enclosing aluminum
4 and magnesium ions in a chain-like structure (Araújo Melo, Ruiz et al. 2002). This tetrahedral
5 arrangement extends throughout the chain and forms channels through the structure (Murray
6 1999). Due to its exceptional structural properties, attapulgite has been selected as a support which
7 has been loaded with the Cs salt of iron substituted tungstophosphate. The resultant hybrid material
8 shows excellent results for plastic degradation reactions and produces a high amount of liquid fuel.
9 Moreover, the synthesized catalysts distinctly affect the pyrolysis temperature and thus cracking
10 process starts at 310 °C that is significantly lower than non-catalytic cracking at 375 °C. Therefore,
11 the prepared hybrid materials are remarkably effective for conversion of waste plastic materials
12 into value added chemicals.
13
14
15
16
17
18
19
20
21
22
23
24
25

26 **Materials and Methods**

27 **Materials**

28
29
30
31
32 Sodium tungstate dihydrate (98 %), disodium hydrogen phosphate (98 %), iron nitrate
33 nonahydrate (99 %), cesium chloride (99 %) and acetic acid (99.5 %) were supplied by Sigma
34 Aldrich. All chemicals were used as received without further purification unless otherwise stated.
35
36
37
38
39 Attapulgite clay was obtained from Ahmad Saeed & Co Pvt Ltd. Low-density polyethylene pellets
40 (20 µm thickness) were purchased from the local market.
41
42
43

44 **Methods**

45 **Synthesis of Cs salt of iron substituted tungstophosphate (Fe-POM)**

46
47
48 Iron substituted Keggin tungstophosphate was synthesized by a simple method as reported
49 in the literature (Simões, Conceição et al. 1999). Briefly, 15.156 mmol (5 g) of sodium tungstate
50 ($\text{Na}_2\text{WO}_4 \cdot 2\text{H}_2\text{O}$) and 1.38 mmol (0.246 g) of disodium hydrogen phosphate ($\text{Na}_2\text{HPO}_4 \cdot 12\text{H}_2\text{O}$)
51
52
53
54
55
56
57
58
59
60

1
2
3 were dissolved in 31 mL of deionized water. Then, 1.82 mmol (0.735 g) of ferric nitrate
4
5 ($\text{Fe}(\text{NO}_3)_3 \cdot 9\text{H}_2\text{O}$) were added to the above mixture, and pH was adjusted to 4.8 with glacial acetic
6
7 acid. The resultant mixture was heated to 80-85 °C, filtered if needed, and then 6.82 mmol of
8
9 cesium chloride (CsCl) dissolved in 5 mL of deionized water was added to this mixture dropwise.
10
11 The solution was cooled to room temperature and 150 mL of ethanol was added as an antisolvent.
12
13 The resultant solid was separated and dissolved in 60 mL of water at 60 °C and recrystallized using
14
15 ethanol, filtered, washed many times with ethanol, and dried at 100 °C for 10 hours. For
16
17 simplification, the product ($\text{Cs}_6[\text{FePW}_{11}\text{O}_{39}] \cdot 12\text{H}_2\text{O}$) was abbreviated as Fe-POM.
18
19
20

21 **Synthesis of Fe-POM/Attapugite Composites**

22
23
24 A series of catalysts were prepared by impregnating with different concentrations (10, 30
25
26 and 50 wt.% relative to attapulgite) of Fe-POM as follows; aqueous suspension of attapulgite clay
27
28 (1 g) was prepared in 50 mL of water. Then, an aqueous solution of the calculated amount of
29
30 $\text{Cs}_6[\text{FePW}_{11}\text{O}_{39}] \cdot 12\text{H}_2\text{O}$ was added into it under constant stirring followed by heating till complete
31
32 evaporation of water. Finally, the composites were dried in an oven at 110 °C (overnight). The
33
34 synthesized composites were symbolized as Fe-POM-10, Fe-POM-30, and Fe-POM-50
35
36 corresponding to attapulgite impregnated with 10, 30, and 50% of $\text{Cs}_6[\text{FePW}_{11}\text{O}_{39}] \cdot 12\text{H}_2\text{O}$.
37
38
39

40 **Cracking Experiment**

41
42
43 Polyethylene (PE) cracking experiment was performed by batch operation using apyrex
44
45 glass reactor (280 mm x 50 mm) as shown in Fig. 1. PE pellets were mixed with the catalyst in a
46
47 weight ratio 20:1 and placed in the reactor for catalytic cracking. Heating of reactor was done in
48
49 two steps: in the former step, it was heated at 2 °C /min to 120 °C under the flow of nitrogen (30
50
51 ml/min) to remove any adsorbed water molecules however in the latter, N_2 supply was
52
53 disconnected and the temperature was increased to cracking temperature (heating rate 5 °C/min).
54
55
56

The experiment was carried out up to three hours. Liquid products and solid residue were weighed directly, however, the amount of gaseous products was determined indirectly by measuring the difference in weight of both liquid products and solid residues from the total weight of PE feed. Total polymer conversion was estimated by the ratio of polymer converted to liquid fuel and the amount of sample fed initially. Liquid hydrocarbons were analyzed by a Gas Chromatograph-Mass Spectrometer (GC-MS QP2010S) using the ZB-5 MS column with dimensions of $30\text{ m} \times 0.32\text{ mm} \times 0.25\text{ }\mu\text{m}$.

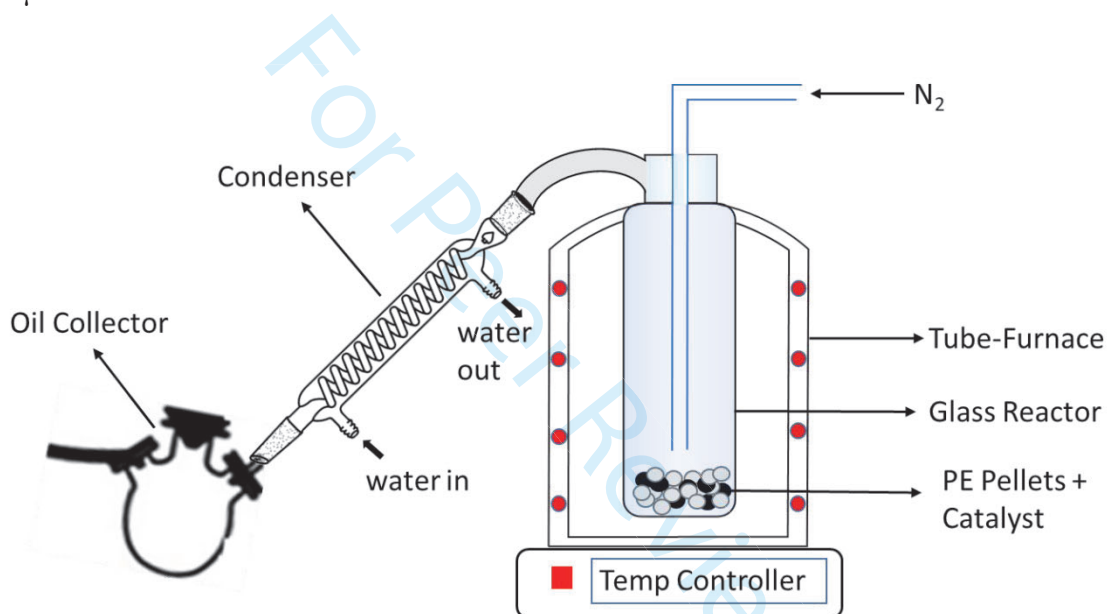


Figure 1: Schematic diagram for set up used for PE cracking experiments.

Characterization Techniques

Characterization of synthesized catalysts was accomplished by various analytical techniques like Fourier Transform Infrared (FTIR) spectroscopy, Powder X-ray Diffraction (PXRD), Scanning Electron Microscopy and Energy-dispersive X-ray spectroscopy (SEM-EDX), and Thermogravimetric analysis (TGA). FTIR spectroscopy was used to identify functional groups with the help of an FTIR Spectrometer (model 41630 by Agilent technology) operating in the ATR

1
2
3 mode. Spectra were recorded at room temperature (4 cm^{-1} resolution, 256 scans/sample). TGA was
4 performed on Netzsch STA 409 instrument: *approx.* 20 mg sample was placed in alumina crucibles
5 and the temperature program was set to rise at a rate of $10\text{ }^{\circ}\text{C}/\text{min}$ upto $1000\text{ }^{\circ}\text{C}$ in the argon
6 environment (flow rate: $60\text{ ml}/\text{min}$). The surface morphology of prepared composites was
7 examined by an XL30 ESEM instrument. Gold targets were used for the pre-coating of samples
8 by a Polaron SC7640 sputter coater. The elemental composition of the samples was obtained with
9 the help of INCA X-Act EDX detector. The crystalline structure of prepared composites was
10 evaluated by PXRD performed on a PANalytical XPERT-PRO system working at 40 kV and 40
11 mA utilizing $\text{Cu K}\alpha$ radiation. The scanning rate was set at 0.02° over 2θ range of 5° - 85° . Liquid
12 products were analyzed by a GCMS-QP2010S instrument using the ZB-5 MS column ($30\text{ m} \times 0.32$
13 $\text{mm} \times 0.25\text{ }\mu\text{m}$) under flow of He gas. GC and MS conditions were as follows: Initial GC oven
14 temperature was kept at $40\text{ }^{\circ}\text{C}$ for 1 min, then heated to $310\text{ }^{\circ}\text{C}$ at a heating rate of $3\text{ }^{\circ}\text{C}/\text{min}$ and
15 held constant for 30 min. The temperature of the injector was maintained at $280\text{ }^{\circ}\text{C}$ while the
16 detector was held at $310\text{ }^{\circ}\text{C}$. EI ionization mode was used to record mass m/z from 30 to 500. Ion
17 source and interface temperatures were kept at $180\text{ }^{\circ}\text{C}$ and $250\text{ }^{\circ}\text{C}$, respectively. All compounds
18 were identified from NIST/EPA/NIH MS Library.
19
20
21
22
23
24
25
26
27
28
29
30
31
32
33
34
35
36
37
38
39
40
41
42
43

44 **Results and Discussion**

45 **Characterization of catalysts**

46 **FTIR**

47
48
49
50
51
52 FTIR spectrum (Fig. 2) of attapulgite clay exhibited characteristic asymmetric vibrations
53 at 920 and 800 cm^{-1} corresponding to Si–O–H and Al–O–Si bonds, respectively. A shoulder peak
54
55
56
57
58
59
60

1
2
3 at 1193 cm^{-1} is ascribed to Si–O–Si bond in clay (MENDELOVICI 1973, Araújo Melo, Ruiz et al.
4
5 2002). The vibrational band at 1600 cm^{-1} is attributed to coordinated water molecules (Fig. 2). Fe-
6
7 POM/attapulgite clay samples exhibit only a few characteristic vibration bands of POM. FTIR
8
9 spectrum of bulk Fe-POM shows typical asymmetric vibrations for P–O_a–W, W=O_d, W–O_b–W
10
11 bridges between corner-sharing WO₆ octahedra, and W–O_c–W bridges between edge-sharing WO₆
12
13 octahedra at 1084, 982, 895 and 789 cm^{-1} , respectively (Rocchiccioli-Deltcheff, Fournier et al.
14
15 1983, Shah, Mujahid et al. 2012). W–O–Fe vibrations are located at 666 cm^{-1} (Gamelas, Soares et
16
17 al. 2003). In case of 50 % POM/attapulgite, only P–O_a–W and W–O_c–W stretching vibrations can
18
19 be seen at 1080 and 789 cm^{-1} , which are characteristic of Fe-POM Keggin structure. However,
20
21 W=O_d and W–O_b–W vibrations of Fe-POM structure located at 982 and 895 cm^{-1} are not obvious
22
23 due to overlapping with the strong bands of silica present in clay's structure.
24
25
26
27
28
29
30
31
32
33
34
35
36
37
38
39
40
41
42
43
44
45
46
47
48
49
50
51
52
53
54
55
56
57
58
59
60

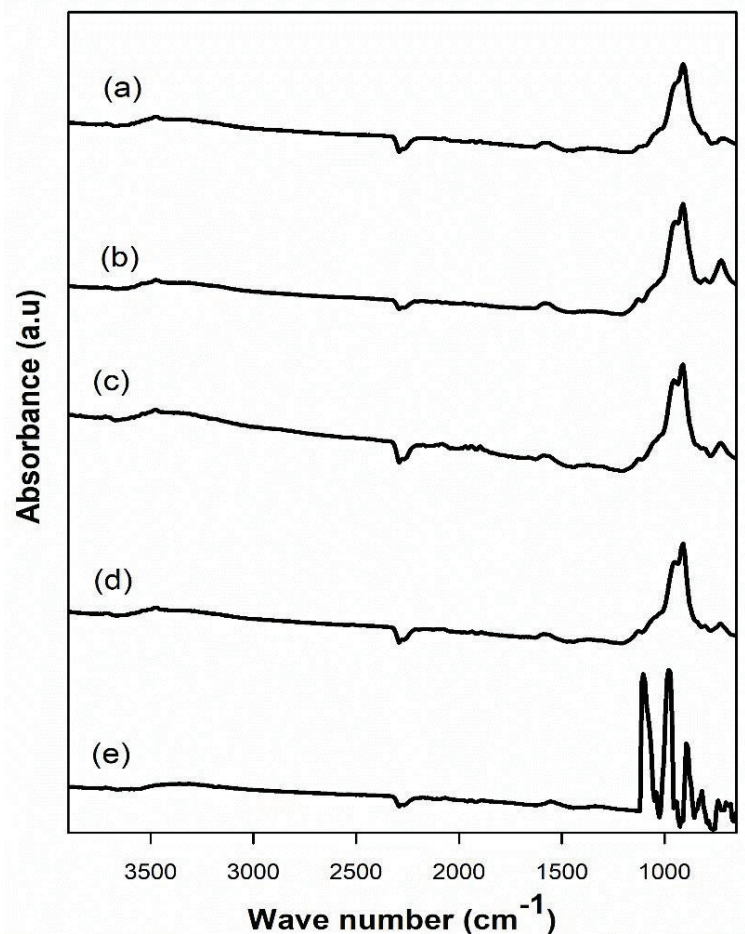
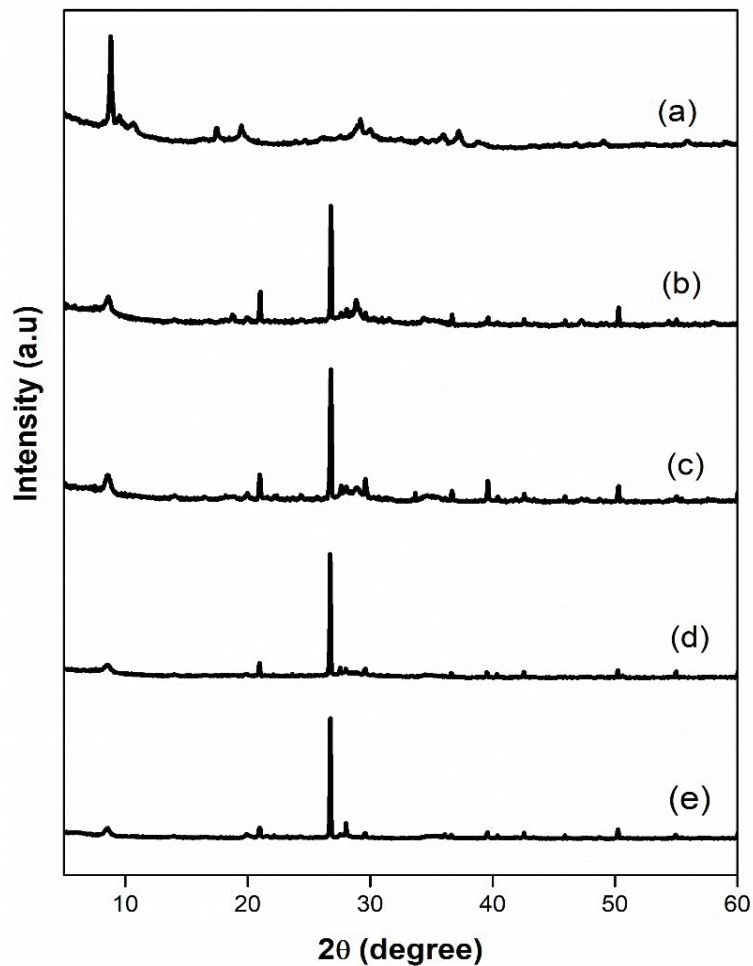


Figure 2: FT-IR spectra of (a) Attapulgite, (b) Fe-POM-50, (c) Fe-POM-30, (d) Fe-POM-10, and (e) Fe-POM samples.

XRD

Attapulgite clay exhibited a high degree of crystallinity as shown in Fig. 3. The diffraction peak observed at 2θ values of 8.5° , 20.2° , and 35.0° are ascribed to basal space of attapulgite framework (PDF No. 02-0018). The peaks located at 2θ values 13° , 16.4° , 20.8° , and 50.1° correspond to silica layers of the clay. The most intense peak corresponding to quartz (PDF No. 33-1161) impurities is located at $2\theta = 26.8^\circ$ (Shepard, Christ et al. 1969, Araújo Melo, Ruiz et al. 2002, Suki, Azahari et al. 2013). XRD patterns of Fe-POM exhibits a cubic crystalline phase that is characteristic of Keggin tungstophosphate (Dias, Caliman et al. 2004, Zhang, Yue et al. 2013).

1
2
3 Diffraction patterns of Fe-POM/attapulgite clay composites present all the characteristic peaks of
4 attapulgite but only a few diffraction peaks of Fe-POM Keggin structure. Attapulgite impregnated
5 with 50 % Fe-POM exhibit characteristic peak of Fe-POM at 2θ value of 8.3° but in 10 % and
6
7
8 with 50 % Fe-POM exhibit characteristic peak of Fe-POM at 2θ value of 8.3° but in 10 % and
9
10 30 % Fe-POM /clay samples this peak is masked by intense diffraction peaks of silica present in
11
12 clay structure.
13
14



1
2
3 **Figure 3:** Powder XRD patterns of (a) Fe-POM, (b) Fe-POM 50, (c) FePOM-30, (d) Fe-POM
4
5 10 and (e) Attapulgite.
6
7

8 TGA

9
10 Thermogravimetric analysis of Fe-POM, attapulgite, and Fe-POM impregnated
11 attapulgite-composites is shown in Fig. 4. TGA data collected for attapulgite exhibited weight loss
12 in four distinct steps. The first two steps are attributed to dehydration and the next two steps
13 correspond to dehydroxylation. During the first step, which starts at ~ 50 °C, physisorbed water
14 molecules are lost (4 wt.%). The second step (located at 245 °C) corresponds to the loss of hydrated
15 water molecules (~ 2 %). The last two steps are complex comprising overlying weight loss steps.
16 The third step is related to two concurring reactions occurring at 450 and 495 °C (comprising
17 weight loss of ~ 4 %). The last step is also completed in two steps occurring at 786 and 820 °C
18 (weight loss ~ 3 %). Nagata et al. have also proposed that the dehydration and dehydroxylation of
19 attapulgite take place in a series of steps (Vágvölgyi, Daniel et al. 2008). These steps are ascribed
20 to the loss of (i) adsorbed water molecules (ii) water molecules of hydration (iii) coordinated water
21 molecules and (iv) the loss of water molecules through dehydroxylation.
22
23
24
25
26
27
28
29
30
31
32
33
34
35
36
37

38 Fe-POM showed a weight loss of 6 % upto 250 °C that was ascribed to water molecules of
39 crystallization and no further noticeable weight loss was observed upto 1000 °C. Fe-
40 POM/attapulgite composites also exhibited thermal behavior analogous to attapulgite clay, the
41 weight loss observed during thermal analysis could be ascribed to the loss of coordinated H₂O
42 molecules and dehydroxylation of silica sheets in attapulgite. However, compared to attapulgite,
43 Attapulgite impregnated with Fe-POM exhibited reduced weight loss in the dihydroxylation phase
44 and this weight loss kept on reducing by increasing the amount of Fe-POM. Attapulgite
45 impregnated with 50 % Fe-POM showed least weight loss during this dehydroxylation step due to
46
47
48
49
50
51
52
53
54
55
56
57

reduced percentage of attapulgite clay (from 100 to 50 %) and increased percentage of Fe-POM (from 0 to 50 %) compared to bare attapulgite, Fe-POM did not lose any water in this region.

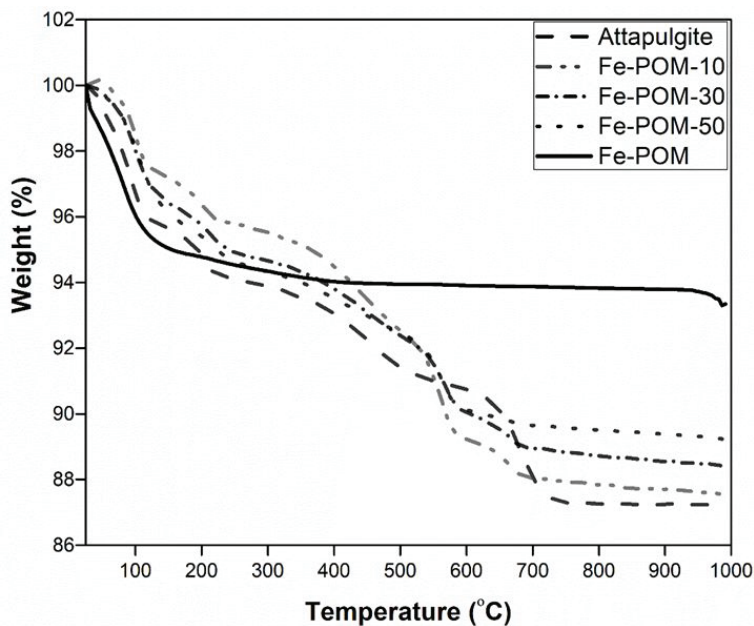
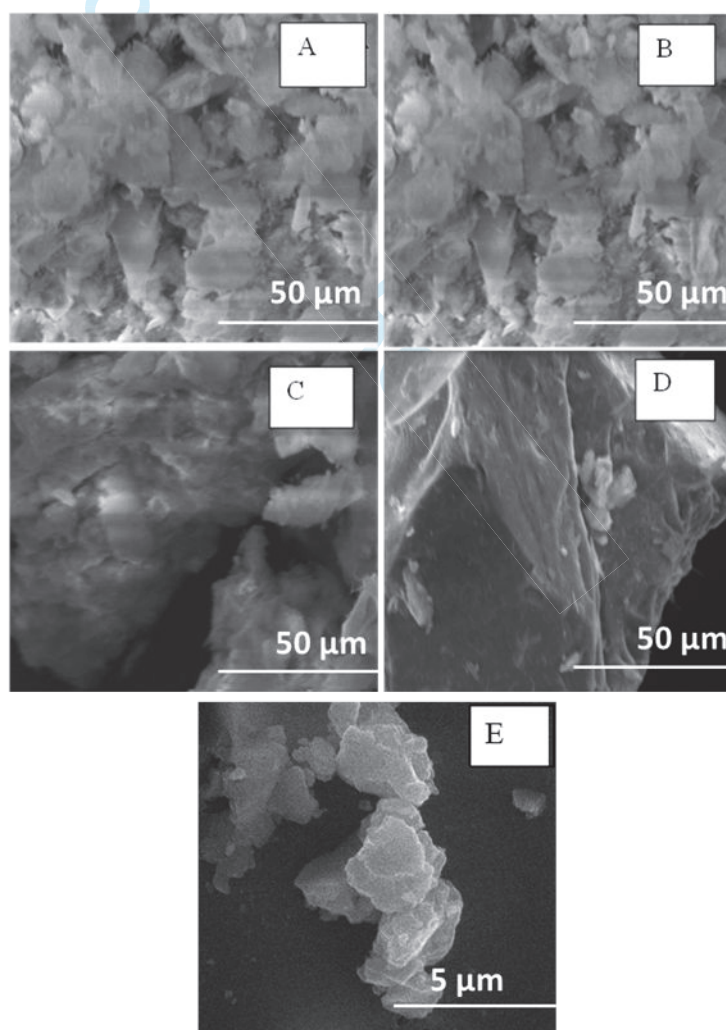


Figure 4: Thermal gravimetric analysis of Fe-POM/attapulgite composites.

SEM-EDX analysis

SEM analysis was conducted to investigate the morphology of prepared catalysts. Attapulgite clay showed crystalline morphology as can be seen in Fig. 5. Fe-POM exhibited a cubic crystalline structure as reported for cesium and silver salts of Keggin tungstophosphate (Dias, Caliman et al. 2004, Zhu, Gao et al. 2013). However, SEM images of Fe-POM/attapulgite composites did not show this crystalline morphology, indicating the uniform distribution of Fe-POM on the attapulgite surface due to the interaction of Fe-POM particles with the clay. Another distinct change in the morphology of Fe-POM/attapulgite composites was the change in the luster of pure attapulgite and Fe-POM loaded attapulgite. Fe-POM impregnated attapulgite samples were more lustrous compared to pure attapulgite. Furthermore, EDX analysis was performed to

1
2
3 determine the elemental composition of these composite materials. EDX analysis of attapulgite
4 shows that the major components of attapulgite are Mg-Al silicate, while iron and titanium are
5 present in trace amounts (Araújo Melo, Ruiz et al. 2002). EDX spectrum of Fe-POM/attapulgite
6 composites revealed that in addition to Mg-Al silicate, tungsten and cesium were also present,
7 confirming the successful loading of Fe-POM on the attapulgite substrate. Moreover, the weight
8 percentage of W and Cs increased by increasing the percentage of Fe-POM. The highest
9 percentage of W and Cs were observed for the 50 % Fe-POM loaded attapulgite composite.
10
11
12
13
14
15
16
17
18
19 Atomic and weight percentages of elements found in all composites are shown in Table S1.



1
2
3 **Figure 5:** SEM images of (A) Fe-POM-50, (B) Fe-POM-30, (C) Fe-POM-10 and
4
5 (D) attapulgite clay.
6
7

8 **Thermal Catalytic Cracking of Polyethylene**

9

10
11 The results of polyethylene cracking in the absence and presence of catalysts are
12 summarized in Table 1. Thermal cracking took place at a very high temperature (375 °C) while in
13 presence of catalysts the cracking temperature was dropped to a great extent. However, various
14 catalysts showed different behavior for the cracking of polyethylene. Fe-POM exhibited lesser
15 yield of liquid oil products and the cracking started at a higher temperature i.e., 350 °C.
16 Impregnation of Fe-POM on attapulgite clay decreased the cracking temperature to 310 °C and
17 enhanced the liquid yield by large amounts. At the same time, the amount of residue was lowered
18 considerably. The liquid yield was enhanced by increasing the amount of Fe-POM loading. 50 %
19 Fe-POM impregnated attapulgite produced 82 % liquid hydrocarbons, while solid residue was
20 reduced to ≤ 2 %. On the other hand, pure attapulgite produced 72 % liquid oil that was far less
21 than the Fe-POM/clay composite samples. POM impregnated on attapulgite creates extra Brønsted
22 acid sites that synergistically enhance catalyst activity for cracking of polyethylene. The
23 enhancement in catalyst acidity would have reduced the cracking temperature and degraded
24 heavier hydrocarbons into smaller ones. PE cracking reactions proceed over the Bronsted acidic
25 sites, as described earlier and therefore with increasing acidic sites the temperature required for
26 cracking decreases (Aydemir and Sezgi 2013). Moreover, recycled 50 % Fe-POM/attapulgite
27 sample exhibited negligible activity loss when applied for LDPE cracking that proved it to be a
28 truly heterogeneous catalyst.
29
30
31
32
33
34
35
36
37
38
39
40
41
42
43
44
45
46
47
48
49
50
51
52
53
54
55
56
57
58
59
60

Table1: Percentage yield of degradation products over various catalysts

Catalyst	Cracking temperature (°C)	Liquid Oil (%)	Gas (%)	Residue (%)
No Catalyst	375	68	10	22
Fe-POM	350	74.67	15.83	9.5
Attapulgate	310	72.7	17.3	10
Fe-POM-10	310	78.4	16.5	5.1
Fe-POM-30	310	80.1	16.7	3.2
Fe-POM-50	310	82.0	15.9	2.1
Recycled Fe-POM-50	310	81.8	15.8	2.4

3.2.1 Composition of liquid Products

The oil fraction obtained by PE cracking was analyzed by GC-MS. Every single peak in the chromatogram corresponded to a specific compound. The molecular weight and structure of these compounds were identified by mass spectrometer. It was found that the oil acquired over all prepared catalysts contained hydrocarbons distribution between C₅–C₂₁ (Fig. 6). Nearly 60 % hydrocarbons comprised of petroleum fractions (C₅–C₁₂), while ≥ 35 % fractions were Kerosene-like hydrocarbons (C₁₃–C₁₈). High molecular weight hydrocarbons (C₁₉–C₂₁) were ≤ 5 %. All the tested catalysts shifted the product distribution towards lower hydrocarbons and the effect was most profound in oil obtained using 50 % Fe-POM/attapulgate sample. Although, C₅–C₈ are produced in enormous amounts in oil obtained using 50 % POM loaded sample but the maximum is observed for C₉–C₁₀ hydrocarbon fraction. On the contrary, Fe-POM gave maximum distribution of C₁₀–C₁₃ fractions, while oil obtained by thermal cracking showed the maximum at C₁₂–C₁₄ fractions (Fig. 6).

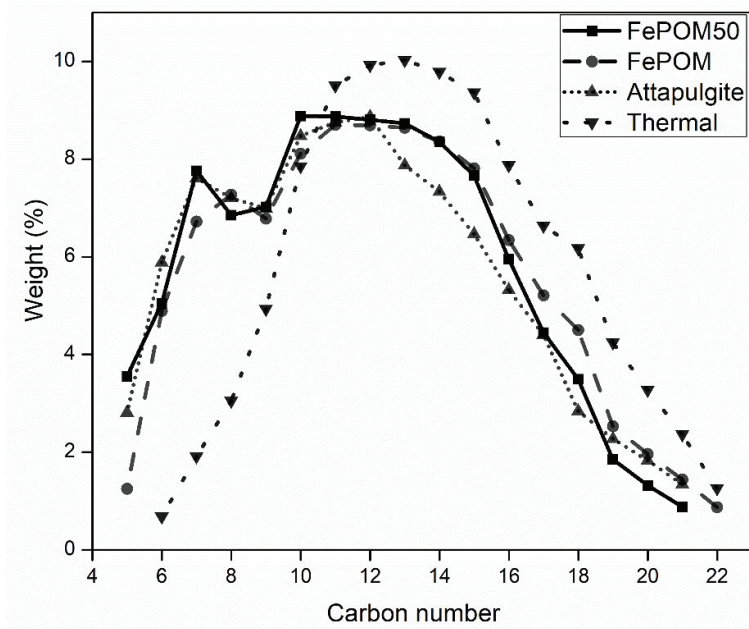


Figure 6: Comparison of distribution of carbon number for various oil samples obtained by thermal, Fe-POM, attapulgite and 50 % Fe-POM/attapulgite catalysts.

Detailed GC-MS analysis revealed that oil produced by catalytic cracking contained mainly aliphatic hydrocarbons (paraffins and olefins). The relative abundance of paraffins and olefins produced by different catalysts are given in Table S-2 (Supplementary file). Among the lower hydrocarbons (C_5 – C_{12}), olefins were more abundant, while in case of heavier hydrocarbons paraffins were prominent. Non-catalytic oil produced a higher percentage of paraffinic hydrocarbons (Table 2), as non-catalytic degradation occurred at a higher temperature, which favors paraffin formation (Rahimi and Karimzadeh 2011). The formation of olefins during non-catalytic and catalytic cracking is also explained by Haag-Dessau mechanism (Kotrel, Knözinger et al. 2000). For catalytic cracking, Si/Al ratio also affects the olefin and paraffin distribution (Yoshimura, Kijima et al. 2001, Han, Lee et al. 2004, Wei, Liu et al. 2005). The maximum percentage of olefin was achieved over 50% Fe-POM/attapulgite catalyst that could be attributed

to the creation of protonic acidified sites (from Fe-POM) and incorporation of Si and Al (from attapulgite) in catalyst. However, no aromatic compounds could be detected in oil samples, the exclusion of aromatics is of great importance from environmental point of view (Artetxe, Lopez et al. 2012). Thus, the prepared catalysts Fe-POM/attapulgite could be regarded as an efficient and cost-effective catalysts for degradation of waste polymeric materials.

Table 2: Product Distribution in oil obtained by different catalysts.

Catalyst	Carbon number	Weight Percent (%)	
		Alkanes	Alkenes
No Catalyst	C ₅ –C ₁₂	19.1	16.62
	C ₁₃ –C ₁₈	21.35	21.20
	>C ₁₈	14.67	----
Fe-POM	C ₅ –C ₁₂	24.85	26.18
	C ₁₃ –C ₁₈	25.04	16.09
	>C ₁₈	6.80	----
Fe-POM-50	C ₅ –C ₁₂	27.03	28.79
	C ₁₃ –C ₁₈	23.83	14.79
	>C ₁₈	4.05	----
Attapulgite	C ₅ –C ₁₂	25.77	28.38
	C ₁₃ –C ₁₈	27.37	12.47
	>C ₁₈	5.44	----

Conclusion

This research reports the synthesis and characterization of iron-substituted tungstophosphate (Fe-POM) impregnated attapulgite clay using various concentrations of Fe-POM (10 %, 30 % & 50 %). The synthesized materials have been successfully characterized by

1
2
3 FTIR, XRD and SEM-EDX analysis. TGA explains the thermal stability of these composite
4 materials. Fe-POM impregnated attapulgite composites have been used as catalysts for polyethylene
5 cracking. The synthesized composite materials exhibit extraordinary performance for the
6
7 conversion of polyethylene to lower hydrocarbons, hence the yield of fuel oil was enhanced to a
8 considerable extent. By increasing the amount of Fe-POM loading, oil yield enhances and
9
10 therefore maximum oil yield is exhibited by 50 % Fe-POM/attapulgite sample. Furthermore, these
11
12 composites also lower the pyrolysis temperature, hence make the cracking process economical.
13
14 Moreover, valuable hydrocarbons have been recovered from waste polymeric materials by
15
16 prepared catalysts for transportation fuels, suggesting the applicability of these catalysts for energy
17
18 recovery from plastic waste along with the effective pollution control of the environment.
19
20
21
22
23
24
25
26

27 **Acknowledgement**

28
29 Higher Education Commission of Pakistan is greatly acknowledged for the grant of Indigenous
30
31 PhD Scholarship (PIN# 213-66412-2PS2-074). We are also thankful to Higher Education
32
33 Commission for NRPU project grant (6776/NRPU/R&D/HEC) to complete this research work.
34
35
36

37 **Supplementary material**

38
39 GC-MS spectra, peak identification table and EDS elemental analysis is provided in supplementary
40
41 material file.
42
43
44

45 **Conflict of interest**

46
47 The authors declare that they have no conflict of interest.
48
49
50

51 **8. References**

1
2
3 Aguado, J., D. P. Serrano, G. S. Miguel, J. M. Escola and J. M. Rodríguez (2007). "Catalytic
4 activity of zeolitic and mesostructured catalysts in the cracking of pure and waste polyolefins."
5

6 Journal of Analytical and Applied Pyrolysis **78**(1): 153-161.
7

8
9 Akpanudoh, N. S., K. Gobin and G. Manos (2005). "Catalytic degradation of plastic waste to liquid
10 fuel over commercial cracking catalysts: effect of polymer to catalyst ratio/acidity content."
11

12 Journal of Molecular Catalysis A: Chemical **235**(1): 67-73.
13
14

15 Araújo Melo, D. M., J. A. C. Ruiz, M. A. F. Melo, E. V. Sobrinho and A. E. Martinelli (2002).
16

17 "Preparation and characterization of lanthanum palygorskite clays as acid catalysts." Journal of
18 Alloys and Compounds **344**(1): 352-355.
19
20
21

22 Artetxe, M., G. Lopez, M. Amutio, G. Elordi, J. Bilbao and M. Olazar (2012). "Light olefins from
23 HDPE cracking in a two-step thermal and catalytic process." Chemical engineering journal **207**:
24 27-34.
25
26
27
28
29

30 Attique, S., M. Batool, M. Yaqub, O. Goerke, D. H. Gregory and A. T. Shah (2020). "Highly
31 efficient catalytic pyrolysis of polyethylene waste to derive fuel products by novel
32 polyoxometalate/kaolin composites." Waste Management & Research **38**(6): 689-695.
33
34
35
36

37 Aydemir, B. and N. A. Sezgi (2013). "Alumina and Tungstophosphoric Acid Loaded Mesoporous
38 Catalysts for the Polyethylene Degradation Reaction." Industrial & Engineering Chemistry
39 Research **52**(44): 15366-15371.
40
41
42
43

44 Bobek-Nagy, J., N. Gao, C. Quan, N. Miskolczi, D. Rippel-Pethő and K. Kovács (2020). "Catalytic
45 co-pyrolysis of packaging plastic and wood waste to achieve H₂ rich syngas." International Journal
46 of Energy Research **44**(13): 10832-10845.
47
48
49
50
51

1
2
3 Chai, Y., M. Wang, N. Gao, Y. Duan and J. Li (2020). "Experimental study on
4 pyrolysis/gasification of biomass and plastics for H₂ production under new dual-support catalyst."
5 Chemical Engineering Journal **396**: 125260.
6
7

8
9
10 Dias, J. A., E. Caliman and S. C. Loureiro Dias (2004). "Effects of cesium ion exchange on acidity
11 of 12-tungstophosphoric acid." Microporous and Mesoporous Materials **76**(1): 221-232.
12
13

14 Gaca, P., M. Drzewiecka, W. Kaleta, H. Kozubek and K. Nowinska (2008). "Catalytic degradation
15 of polyethylene over mesoporous molecular sieve MCM-41 modified with heteropoly
16 compounds." Polish Journal of Environmental Studies **17**(1): 25.
17
18

19 Gamelas, J. A. F., M. R. Soares, A. Ferreira and A. M. V. Cavaleiro (2003). "Polymorphism in
20 tetra-butylammonium salts of Keggin-type polyoxotungstates." Inorganica Chimica Acta **342**: 16-
21 22.
22
23

24 Han, S. Y., C. W. Lee, J. R. Kim, N. S. Han, W. C. Choi, C.-H. Shin and Y.-K. Park (2004).
25 Selective Formation of Light Olefins by the Cracking of Heavy Naphtha. Carbon Dioxide
26 Utilization for Global Sustainability: Proceedings of the 7th International Conference on Carbon
27 Dioxide Utilization, Seoul, Korea, October 12-16, 2003, Elsevier.
28
29

30 Kotrel, S., H. Knözinger and B. Gates (2000). "The Haag-Dessau mechanism of protolytic
31 cracking of alkanes." Microporous and mesoporous materials **35**: 11-20.
32
33

34 Lin, Y.-H., M.-H. Yang, T.-F. Yeh and M.-D. Ger (2004). "Catalytic degradation of high density
35 polyethylene over mesoporous and microporous catalysts in a fluidised-bed reactor." Polymer
36 degradation and stability **86**(1): 121-128.
37
38

39 Luo, W., Z. Fan, J. Wan, Q. Hu, H. Dong, X. Zhang and Z. Zhou (2021). "Study on the reusability
40 of kaolin as catalysts for catalytic pyrolysis of low-density polyethylene." Fuel **302**: 121164.
41
42
43
44
45
46
47
48

1
2
3 Mastral, J. F., C. Berrueco, M. Gea and J. Ceamanos (2006). "Catalytic degradation of high density
4 polyethylene over nanocrystalline HZSM-5 zeolite." Polymer Degradation and Stability **91**(12):
5
6 3330-3338.
7

8
9
10 MENDELOVICI, E. (1973). "Infrared Study Of Attapulgite And HCl Treated Attapulgite
11
12
13 " Clays and Clay Minerals **Vol. 21**: pp. 115-119.
14

15 Murray, H. H. (1999). Applied clay mineralogy today and tomorrow. Clay Minerals. **34**: 39.
16

17 Patil, L., A. K. Varma, G. Singh and P. Mondal (2018). "Thermocatalytic Degradation of High
18 Density Polyethylene into Liquid Product." Journal of Polymers and the Environment **26**(5): 1920-
19
20 1929.
21
22

23
24 Rahimi, N. and R. Karimzadeh (2011). "Catalytic cracking of hydrocarbons over modified ZSM-
25
26 5 zeolites to produce light olefins: A review." Applied Catalysis A: General **398**(1): 1-17.
27

28
29 Rocchiccioli-Deltcheff, C., M. Fournier, R. Franck and R. Thouvenot (1983). "Vibrational
30 investigations of polyoxometalates. 2. Evidence for anion-anion interactions in molybdenum (VI)
31 and tungsten (VI) compounds related to the Keggin structure." Inorganic Chemistry **22**(2): 207-
32
33 216.
34
35

36
37
38 Saira Attique, M. B., Muhammad Irfan Jalees, Khurram Shehzad., Zakir Khan., Umar Farooq.,
39
40 Fawad Ashraf., Asma Tufail Shah. (2018). "Highly efficient catalytic degradation of low-density
41 polyethylene Using a novel tungstophosphoric acid/kaolin clay composite catalyst." Turkish
42
43 journal of Chemistry(42): p. 684-693.
44
45

46
47 Serrano, D. P., J. Aguado and J. M. Escola (2000). "Catalytic conversion of polystyrene over
48 HMCM-41, HZSM-5 and amorphous SiO₂-Al₂O₃: comparison with thermal cracking." Applied
49
50 Catalysis B: Environmental **25**(2): 181-189.
51
52
53

1
2
3 Shah, A., S. Attique, M. Batool, H. R. Godini and O. Görke (2021). Role of polyoxometalates in
4 converting plastic waste into fuel oil: 333-355.

5
6
7 Shah, A. T., A. Mujahid, M. U. Farooq, W. Ahmad, B. Li, M. Irfan and M. A. Qadir (2012).
8 "Micelle directed synthesis of (C₁₉H₄₂N)₄H₃(PW₁₁O₃₉) nanoparticles and their catalytic
9 efficiency for oxidative degradation of azo dye." Journal of Sol-Gel Science and Technology
10 **63**(1): 194-199.

11
12
13 Shepard, A. O., C. L. Christ, J. C. Hathaway and P. B. Hostetler (1969). "Palygorskite: New X-
14 Ray data1." American Mineralogist **54**(1-2): 198-205.

15
16
17 Simões, M. M. Q., C. M. M. Conceição, J. A. F. Gamelas, P. M. D. N. Domingues, A. M. V.
18 Cavaleiro, J. A. S. Cavaleiro, A. J. V. Ferrer-Correia and R. A. W. Johnstone (1999). "Keggin-
19 type polyoxotungstates as catalysts in the oxidation of cyclohexane by dilute aqueous hydrogen
20 peroxide." Journal of Molecular Catalysis A: Chemical **144**(3): 461-468.

21
22
23 Suki, F. M. M., N. A. Azahari, N. Othman and H. Ismail (2013). "XRD Analysis and Tensile
24 Properties of Attapulgite Clay Filled Polyvinyl Alcohol/Corn Starch Blend Films." Advanced
25 Materials Research **620**: 99-104.

26
27
28 Vágvölgyi, V., L. M. Daniel, C. Pinto, J. Kristóf, R. L. Frost and E. Horváth (2008). "Dynamic
29 and controlled rate thermal analysis of attapulgite." Journal of Thermal Analysis and Calorimetry
30 **92**(2): 589-594.

31
32
33 Wang, J., J. Jiang, Y. Sun, X. Wang, M. Li, S. Pang, R. Ruan, A. J. Ragauskas, Y. S. Ok and D.
34 C. Tsang (2021). "Catalytic degradation of waste rubbers and plastics over zeolites to produce
35 aromatic hydrocarbons." Journal of Cleaner Production **309**: 127469.

1
2
3 Wei, Y., Z. Liu, G. Wang, Y. Qi, L. Xu, P. Xie and Y. He (2005). "Production of light olefins and
4 aromatic hydrocarbons through catalytic cracking of naphtha at lowered temperature." Studies in
5
6 Surface Science and Catalysis **158**: 1223-1230.
7

8
9
10 Yoshimura, Y., N. Kijima, T. Hayakawa, K. Murata, K. Suzuki, F. Mizukami, K. Matano, T.
11
12 Konishi, T. Oikawa and M. Saito (2001). "Catalytic cracking of naphtha to light olefins." Catalysis
13
14 Surveys from Japan **4(2)**: 157-167.
15

16
17 Zhang, L., B. Yue, Y. Ren, X. Chen and H. He (2013). "An aluminum promoted cesium salt of
18
19 12-tungstophosphoric acid: a catalyst for butane isomerization." Catalysis Science & Technology
20
21 **3(8)**: 2113-2118.
22

23
24 Zhu, S., X. Gao, F. Dong, Y. Zhu, H. Zheng and Y. Li (2013). "Design of a highly active silver-
25
26 exchanged phosphotungstic acid catalyst for glycerol esterification with acetic acid." Journal of
27
28 Catalysis **306**: 155-163.
29

Supplementary information for

**Fe-POM/ Attapulgite Composite Materials: Efficient catalysts for plastic
pyrolysis**

Table S1: Weight % and atomic % of elements found in Fe-POM and Fe-POM/Attapulgite composites.

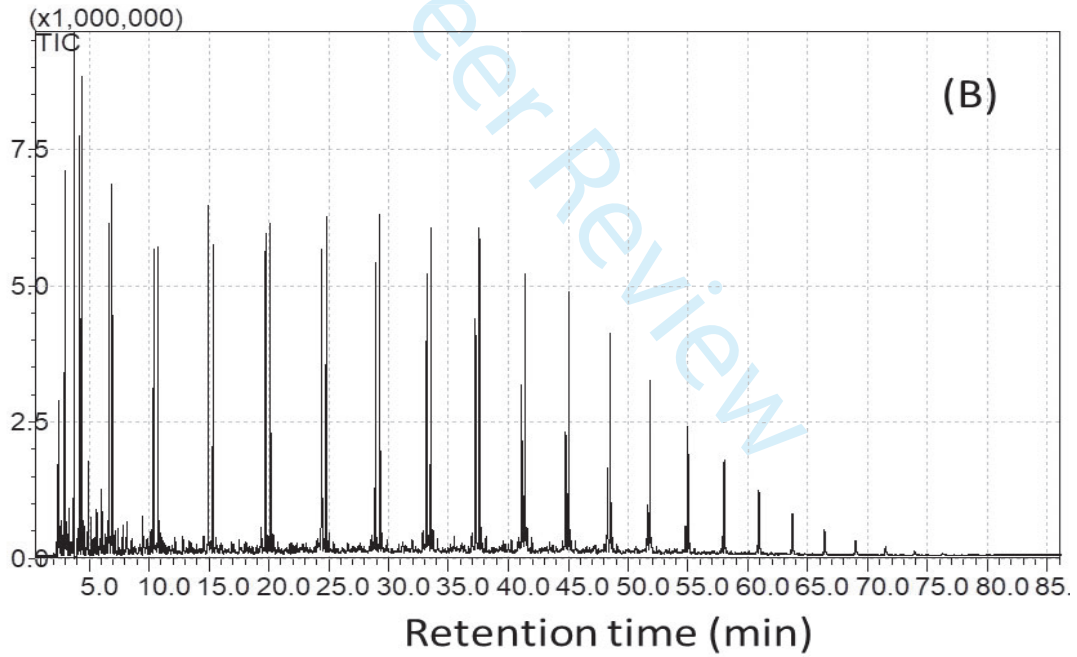
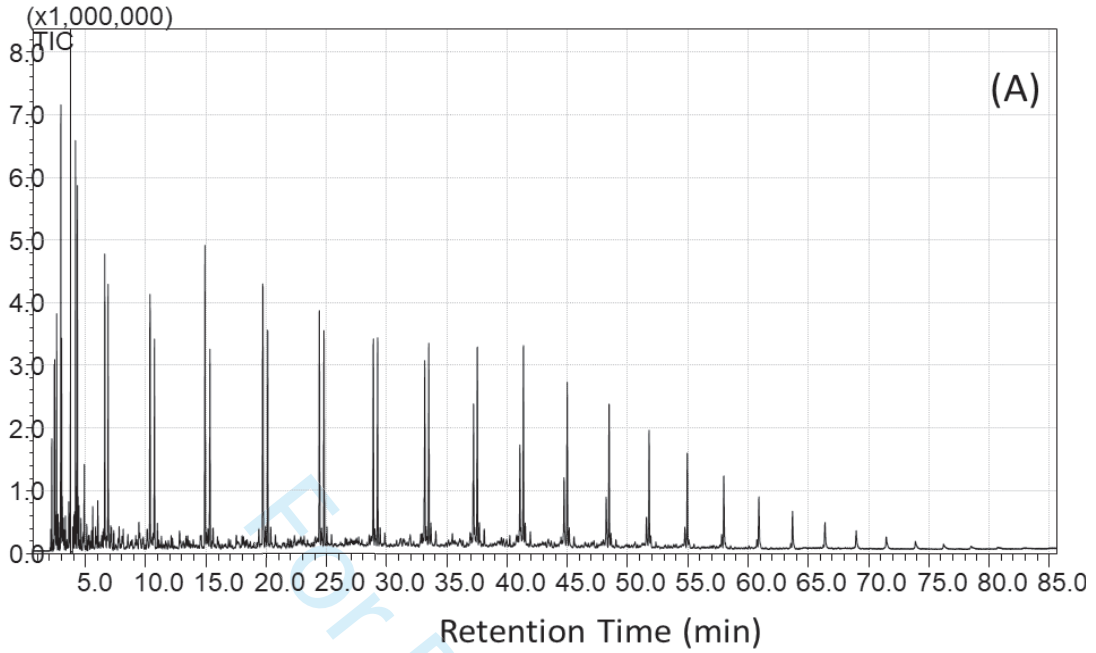
Catalyst	Element	Weight %	Atomic %
Attapulgite	O	62.06	74.45
	Na	0.72	0.60
	Mg	4.24	3.35
	Al	5.67	4.03
	Si	23.93	16.35
	K	0.31	0.15
	Ti	0.28	0.11
	Fe	2.79	0.96
Fe-POM-50	O	42.97	71.90
	Na	0.60	0.70
	Mg	2.96	3.26
	Al	3.53	3.51
	Si	14.30	13.83
	Ca	1.18	0.79
	Fe	1.84	0.88
	Cs	7.59	1.53
Fe-POM-30	W	24.83	3.61
	O	44.21	70.19
	Na	0.53	0.58
	Mg	3.06	3.19
	Al	3.43	3.23

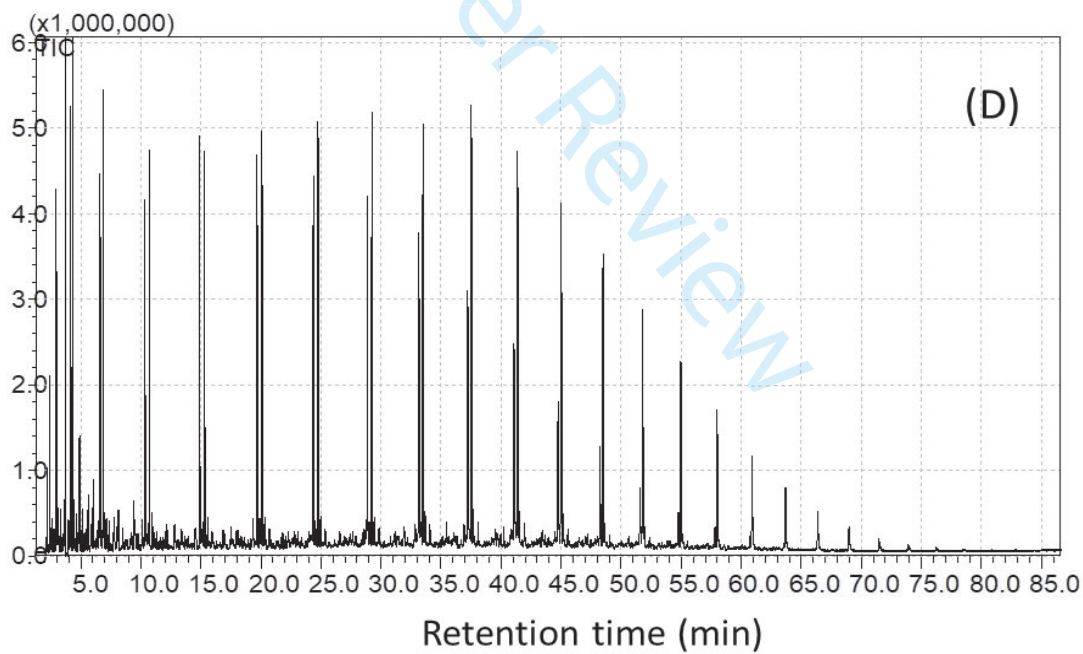
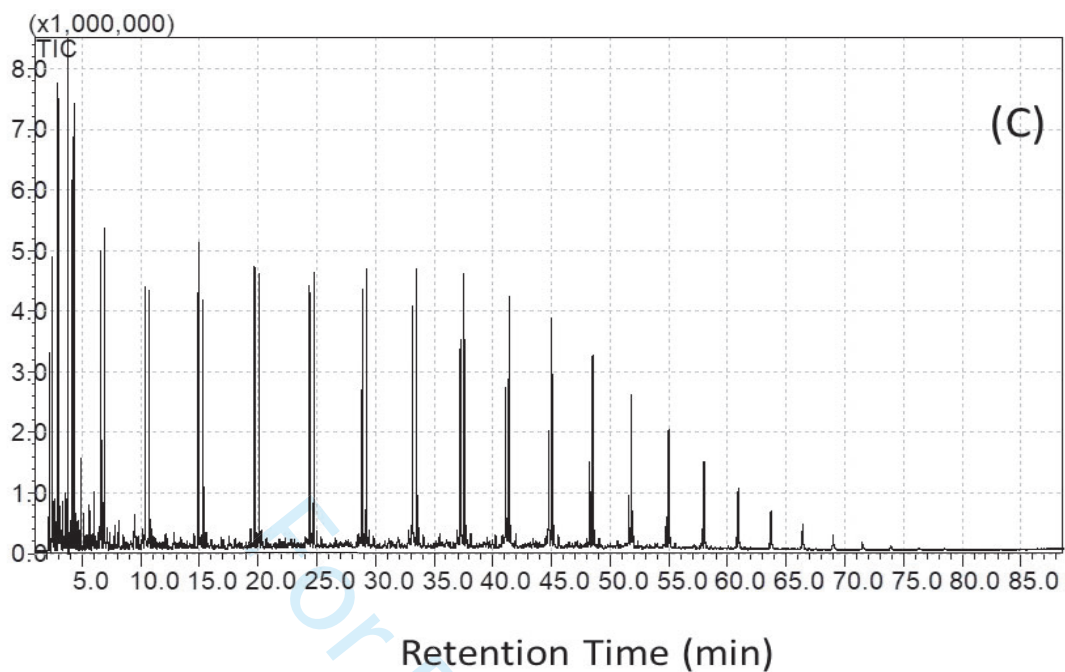
	Si	14.65	13.24
	Ca	1.02	0.64
	Fe	1.85	0.84
	Cs	5.41	1.03
	W	19.69	2.72
Fe-POM-10	O	45.97	72.90
	Na	0.50	0.60
	Mg	2.96	3.26
	Al	3.53	3.51
	Si	14.50	13.83
	Ca	1.18	0.79
	Fe	1.84	0.88
	Cs	4.59	1.23
	W	17.83	2.41

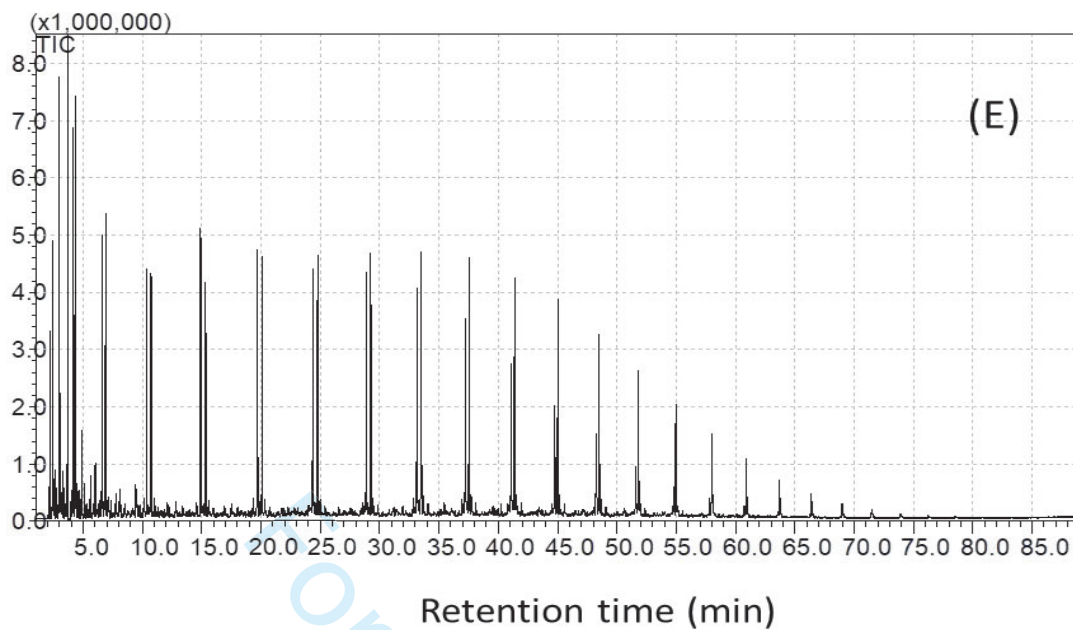
Table S-2: Identification of different compounds in the oil produced by various catalysts by GC-MS Analysis

RT (min)	Peak Name	Relative Abundance (%)			
		No Catalyst	Fe-POM	Attapulgit	Fe-POM-50
2.196	1-Butene-2-methyl	----	0.50	0.96	1.02
2.401	1-Pentene	----	1.10	1.35	1.08
2.430	n-Pentane	----	0.75	1.46	1.45
2.618	1,3-Pentadiene	0.39	--	--	0.38
2.939	1-Hexene	0.29	2.43	2.87	3.04
3.007	n-Hexane	----	1.83	1.99	2.01
3.605	1,4 pentadiene-3-methyl	0.94	0.61	0.45	0.74
4.177	1-Heptene	0.97	2.81	3.17	3.14
4.327	n-Heptane	----	3.25	3.95	3.44

4.84	2-Pentene-4,4-dimethyl	----	0.66	0.62	0.74
6.013	Cyclohexane methylene	1.42	---	---	0.77
6.047	Heptane-3 methylene	1.63	---	---	0.74
6.600	1-Octene	2.51	2.92	3.57	3.10
6.876	n-Octane	2.42	3.61	3.73	3.75
10.349	1-Nonene	4.56	3.31	3.68	3.51
10.718	n-Nonane	3.29	3.47	3.11	3.51
14.900	Cis-3-decene	5.10	4.33	4.10	4.45
15.308	n-Decene	4.40	3.78	3.37	3.83
19.683	2-Undecene	5.12	4.34	4.32	4.46
20.090	n-Undecene	4.80	4.36	3.83	4.41
24.374	1-dodecene	5.04	4.14	4.01	4.23
24.762	n-dodecene	4.98	4.55	4.05	4.63
28.872	1-tridecene	4.89	3.94	3.92	3.98
29.235	n-tridecene	4.89	4.70	3.93	4.75
33.151	3-tetradecene	4.43	3.72	3.45	3.67
33.493	Tetradecane	4.93	4.64	3.88	4.68
37.216	1-Pentadecene	3.50	3.19	2.56	3.05
37.531	n-Pentadecene	4.37	4.62	3.90	4.61
41.074	1-Hexadecene	2.75	2.20	1.60	2.01
41.368	n-Hexadecene	3.88	4.14	3.72	3.94
44.744	1-Heptadecene	2.43	1.51	0.94	1.22
45.012	n-Heptadecane	3.74	3.70	3.10	3.94
48.235	1-Octadecene	1.50	1.26	--	0.87
48.481	n-Octadecane	2.74	3.24	2.84	2.62
51.793	n-Nonadecane	1.04	2.53	2.27	1.85
54.910	Eicosane	2.23	1.96	1.83	1.32
57.91	Henicosane	1.74	1.44	1.34	0.88
60.918	Docosane	1.26	0.87	---	---
63.976	Tricosane	0.82	----	----	----







24 **Figure S1:** GC-MS spectra of oil produced by (A) FePOM, (B) 50% FePOM/Attapulgite, (C)
25 30% FePOM/Attapulgite, (D) 10% FePOM/Attapulgite, and (E) Attapulgite clay.
26
27
28
29
30
31
32
33
34
35
36
37
38
39
40
41
42
43
44
45
46
47
48
49
50
51
52
53
54
55
56
57
58
59
60